

Carbon burnout from the char of a single cylindrical pellet

Mykola M. Zhovmir

*Institute of Renewable Energy
of the National Academy
of Sciences of Ukraine,
Hnat Khotkevych St. 20 A,
02094 Kyiv, Ukraine
Email: mykola.zhovmir@gmail.com*

In countries with limited wood fuel resources, the use of straw for energy should be increased to comply with environmental commitments. Boiler houses burning whole straw bales have limited application because of unfavourable straw logistics and obstacles to their construction in most densely built-up settlements. Straw pellets are more convenient for transportation and safer for storage. Boilers with pellet burning can be operated in fully automatic mode. However, burning straw pellets instead of wood pellets is complicated with increased ash content and lower ash melting temperature. Approaches for low-temperature burning of straw pellets at temperatures below the initial deformation temperature of their ash are of practical interest. At low temperatures, burning is slowing and incomplete burnout with energy loss is possible. The rate of burnout also depends on the form and dimensions of the particle. It was common to accept the rate of carbon burnout as uniform on the reacting surface of the particle.

This work aimed to study the low-temperature carbon burnout from the char of the cylindrical pellets of various lengths and to estimate the energy loss with unburned carbon.

The aim was achieved by the mathematical description of pellet char burning, in which the actual cylindrical char was regarded as the infinite cylinder intersecting with the endless plate. The burnout of fixed carbon was accepted as layered, the carbon burning fronts as infinitely thin, and different rates of carbon burning in radial and axial directions were accepted. An experimental study of the low-temperature burning of fixed carbon from the char of wood and straw pellets was conducted at free air access at 700°C in the furnace, i.e., the temperature around a single pellet was certainly lower than the possible initial deformation temperature of the pellet ash. The duration of carbon burnout from the char of single cylindrical pellets depending on their lengths was studied.

The research findings are as follows. Equations in a dimensionless form, describing changes in the remaining share of unburned fixed carbon in pellet char in time, were deduced analytically. At the experimental burning of single straw pellets, loose particles of ash with no signs of melting formed, but they contained unburned carbon. The share of unburned fixed carbon in ash was 0.016–0.020. The coefficient of determination of calculated and experimental duration of complete burnout of fixed carbon from wood pellet char was $R^2 = 0.96$,

and $R^2 = 0.87\text{--}0.91$ at incomplete burnout from straw pellet char. The most significant scientific result is that for long pellets, the fixed carbon burnout is controlled mainly by its slower burnout rate in the radial direction, and for the shortest pellets by more intensive burnout rate in the axial direction.

The practical value of the results obtained is that the use of shorter pellets, which are characterised by faster burnout, may become purposeful for intensive combustion. Conversely, for slow combustion, and especially with the aim of arranging low-temperature burning of straw pellets, it may be feasible to use longer pellets with extended burnout. In the given conditions of straw pellet burning, the unburned carbon presents in ash, but losses of the pellet energy with unburned carbon were estimated at 0.61–0.72%, which is acceptable for boiler burners.

Keywords: straw pellets, wood pellets, single particle, char burning, fixed carbon burnout, unburned carbon, energy loss

INTRODUCTION

The current task of energy development is to increase renewable energy use, biomass in particular. By joining the European Energy Community, Ukraine accepted commitments to achieve the 11% share of renewable energy in the final energy consumption until 2020. The Energy Strategy of Ukraine for the period until 2035 envisages an increased contribution of renewable energy up to 25%, and the contribution of biomass should reach 4 million tonnes of oil equivalent (mtoe) in 2020 and 11 mtoe in 2035 [1]. According to statistical data, in 2017, the share of renewable energy in the country's energy balance was 4.4% or 3.964 mtoe, and the contribution of biomass and waste was 3.4% or 3.046 mtoe [2]. At the same time, consumption of solid biofuels was 126 941 TJ (3.031 mtoe), and their export was 17 350 TJ (0.414 mtoe) [3].

In Ukraine, technically achievable solid biomass resources for energy usage are estimated at 18 mtoe annually [4], which is sufficient to achieve the goal. Estimations of biomass resources contain the actual portion, which is due to the current level of economic activity, and the virtual portion, i.e., biomass resources that can be obtained only after the organisation of growing and harvesting of energy plants. At the current level of economic activity, about 2 mtoe of wood

and wood waste and 8.6 mtoe of cereal straw and canola stalks can be technically available for energy needs [4]. The harvesting of corn and sunflower stalks is not underway, so there is a necessity for the widespread usage of cereal straw as fuel with limited resources of wood fuel to achieve the goal of biomass contribution to the energy balance.

According to our estimates, 44 boilers with periodic burning of whole straw bales with rated heat output of 150 to 980 kW were operated in Ukraine in 2019, and their total heat output was 25 MW, and annual consumption of baled straw was only near 0.005 mtoe. Such factors as unfavourable logistics of straw, high capital costs of boiler houses with the burning of whole straw bales, inability to build straw warehouses and boiler houses in most cities, and even in small towns or rural settlements because high density of buildings of the Soviet period constrains the use of boilers burning whole straw bales.

These obstacles can be overcome by producing straw pellets and using them as fuel. Pellets are more convenient and safer for transportation and storage allowing complete mechanisation and automation of their usage. Straw pellets can be regarded as a promising fuel for boiler houses in the steppe part of the country. In Ukraine, several straw pellet factories have been built, mainly to export straw pellets as fodder and litter for animals.

Compared to wood, cereal straw has an increased ash content and lower melting temperature characteristics, which can change widely. After determining the ash melting behaviour for 24 samples of wheat and barley straw, the ranges for initial deformation temperature (IDT) were found to be 720–1120°C, softening temperature (SOT) 760–1110°C, hemisphere temperature (HT) 1038–1280°C, and fluid temperature (FT) 1080–1500°C [5]. According to the study of five samples, the softening temperature (SOT) of wheat straw ash was 726–840°C [6].

Burning of straw pellets in retort burners and burners with movable grate was complicated by ash agglomeration, disruption of their work with a significant decrease in heat output and reduced energy efficiency, increased CO emission, which is more expressed for a retort burner [7].

Biagini and Tognotti in [8] showed that in the presence of air, carbon oxidation from wood char was complete at 700°C. This fact indicates the potential possibility for low-temperature burning of wood biomass and encourages finding approaches for low-temperature burning of straw pellets at temperatures below the initial deformation temperature of their ash.

In studies into pellet burning, two approaches can be identified: (1) crushing pellets to small (thermally thin) particles and thermogravimetric study of their thermal destruction and carbon burnout at a relatively slow heating rate [8]; such studies were carried out as to the torch [9, 10] or fluidised bed burning [11]; (2) study into thermal destruction and carbon burnout from larger particles and whole pellets (thermally thick particles) relating to their burning in a fixed fuel bed [12–15].

Researches in the destruction and oxidation of large biomass particles and whole pellets are complex because of the impact of the biomass properties, the content of moisture and ash, and the particle size and shape. In [12], Yang et al. noted that at fixed bed combustion of large biomass particles, 'a temperature gradient over 400°C inside the particles at the front, and significant overlapping of moisture evaporation, devolatilisation and char burnout in the bed-height direction' can develop.

The shape of the burning particles was often considered spherical, which allowed simplifying the mathematical model to one-dimensional. In [13], Lu et al. noted that the spherical mathe-

matical approximation poorly displayed the combustion behaviour for the particle size above a few hundred microns.

In [14], Mehrabian et al. described the mathematical model of thermal conversion of thermally thick biomass particles, which accounts for the shape and size. The biomass particle was divided into four zones: ash, coke, dry fuel, and wet fuel. It has been found that 'the particle with a higher sphericity has the lowest mass loss rate, because the higher sphericity means a smaller surface area to mass ratio'.

Momeni et al. [15] experimentally investigated the effect of the shape of the biomass particle on the rate of its burnout. They determined that for particles with the same volume, cylindrical particles lost their mass faster than spherical particles and the burnout time was shortened by increasing the particle surface area.

In [14], temperature changes on the surface and the centre of a burning wood particle with the diameter of up to 9.5 mm with a moisture content of 6%wt. were studied at high furnace temperature (1000°C). In [16], the burning of pellets (diameter of 8 mm) was studied at furnace temperatures of up to 800°C. These data showed that the temperature in particle cross-section was almost uniform, about 540–550°C, before the time of complete volatile release. It follows that, unlike wet wood particles, at small dry wood particle and pellet burning, carbon burnout began only after the volatile release, and there were only two zones, the coke zone and the ash zone, at carbon burnout.

For practical calculations of pellet combustion, it is interesting to obtain experimental data on the burning rate for the stage of carbon burnout from char, as this stage is largely determining the overall duration of combustion. In [17], Silin et al. studied wood particle and pellet burning in the furnace with free air access, the average rate of carbon burnout from char determined as a rate of mass decrease for the entire period of carbon burnout and attributed it to the particle initial surface area in the assumption that it had a spherical shape. According to them, the carbon burning rate was 2.0 to 2.3 g/(m²·s) at the air speed of 0–0.5 m/s, and according to Palchonok et al. [18], at the air speed of 0.18 m/s, the rate of carbon burning was 4 g/(m²·s).

In well-known works on fuel burning, fuel particles were considered isotropic by default,

and the rate of carbon burnout was considered the same for the entire particle surface. Such an approach is also evident from [13–15], where the difference in the burnout time for spherical and cylindrical particles is explained only by the ratio of mass and surface area.

In [19, 20], the un-uniformity of carbon burnout rate at the surface of pellet char was described. The direct measurements of carbon burnout rate in the radial direction using long defectless wood and straw pellets having a correct cylindrical shape with insulated ends were described in the paper [19].

Having analysed the process of pellets formation in the press with a cylindrical matrix and pressuring rollers, [20] assumed that in the axial (longitudinal) direction the material densification is more significant than in the radial direction, so pellets may be inherent the anisotropic properties. Wendi Guo et al. [21] drew attention to the pellet thermal conductivity anisotropy but studied the effective thermal conductivity of pellets bulk.

It was noted in [20] that carbon burnout from the pellet char occurs both on the cylindrical side surface and on the flat end faces of the pellet char; at the same time, the almost flat fronts of the carbon burning are shifting from the ends towards the middle of the char faster than the cylindrical carbon burning front shifts in the radial direction to the particle axis; the ends of the char are glowing brighter than its cylindrical surface against the background of the furnace glow, which may indicate their higher temperature, and, under almost the same conditions of heat exchange, greater energy release and an increased carbon burning rate on the ends of the pellet char. Based on the above, it was suggested that the rate of carbon burning from the pellet char depends on the directions: is more significant in the axial direction than in the radial. According to the direct measurements using a thin round plate cut from the pellet perpendicular to its longitudinal axis, the carbon burnout rate from the pellet char in the axial direction was 1.7–2 times higher than that in the radial direction for the char of wood pellets, and 1.4–1.5 times higher for the char of straw pellets.

This work aimed to study low-temperature carbon burnout from the char of cylindrical pellets of various lengths and to estimate the energy loss with unburned carbon.

RESEARCH METHODOLOGY

The carbon burnout from the char of wood and straw pellets was regarded at free access of air in a muffle furnace at 700°C, i.e., at the temperature around a single particle which was knowingly below the possible initial deformation temperature of its ash. It was assumed that such low-temperature burning of straw pellets could prevent the agglomeration of ash, but incomplete burnout of fixed carbon could be possible.

The study was carried out in analytical and experimental methods. A mathematical description of burnout of fixed carbon from char of the cylindrical pellet was developed, taking into account different carbon burnout rates in radial and axial directions. The adequacy of the mathematical description was tested by comparing the calculated time of carbon burnout with the corresponding experimentally-found values of burnout of the char of straw and wood pellets of different diameters and lengths.

Analytical method

The initial dimensions of the char were accepted as equal to those of the pellet. This position correlates with the results described in [22] devoted to thermal shrinkage of pellets at pyrolysis in the inert atmosphere, indicating its insignificance at 600–700°C during 30–50 s. The char of a cylindrical pellet (with the diameter $d = 2R_0$ and the length $l = 2\delta_0$) was regarded as a result of the infinite cylinder, with the initial radius R_0 , intersection with the endless plate, with half-thickness δ_0 , see Fig. 1.

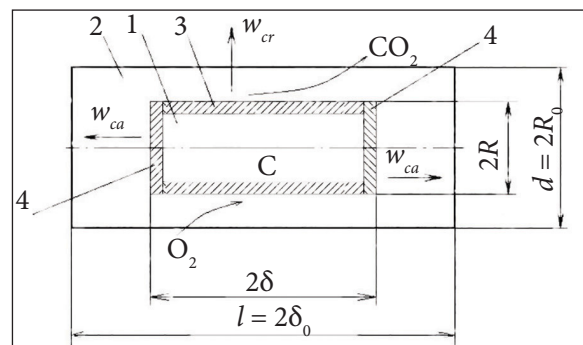


Fig. 1. Scheme to the mathematical description of carbon burnout from the cylindrical pellet char: 1 – char, 2 – ash, 3 – carbon burning front in the radial direction, 4 – carbon burning fronts in the axial direction

At the formulation of the mathematical description, the burnout of fixed carbon from the pellet char was regarded as occurring in an infinitely thin layer shifting the reaction surface beneath the remaining ash. As in [19, 20], the rates of carbon burning were supposed to be constant but different in radial w_{cr} and axial w_{ca} directions because of the pellet anisotropy.

On the reacting surface, the cylindrical front with current radius R , where carbon burning occurred with a shifting of the named front along the radius to the axis of particle, and two flat fronts located at a distance δ from the middle of the char particle, where carbon burning occurred with a shifting of these fronts along the axis to the middle of particle, were distinguished.

Determining geometrical coordinates of carbon burnout fronts in the pellet char

In [19], the differential equation describing the burnout of fixed carbon from the char of the infinite cylindrical pellet with an initial radius R_0 at a constant rate of carbon burning in the radial direction w_{cr} was solved analytically. The equation for determining the time τ during which the cylindrical front of carbon burning will shift from the initial position on the particle surface R_0 to the current radius R was derived:

$$\tau = \frac{\rho_c}{w_{cr}}(R_0 - R), \quad (1)$$

where τ is the time from the beginning of carbon burning from char, s; w_{cr} – the rate of carbon burnout from the char in the radial direction, kg/(m²·s); ρ_c – conditional carbon density in the char, kg/m³.

The conditional carbon density in the char can be defined as the ratio of the fixed carbon mass m_c to the pellet initial volume V [19]:

$$\rho_c = \frac{m_c}{V} = \rho_d(1 - A_d)(1 - V_{daf}), \quad (2)$$

where ρ_d is the density of the dry pellet, kg/m³; V_{daf} is the volatile on a dry ash-free basis, a share of mass; A_d is the ash content on a dry basis, a share of mass.

The current radius R of the cylindrical front of carbon burning at the time τ was determined from the equation (1):

$$R = R_0 - \frac{\tau w_{cr}}{\rho_c}. \quad (3)$$

Dividing the right and left sides of the equation (3) by R_0 , it was converted into a dimensionless form:

$$r = 1 - \frac{\tau w_{cr}}{R_0 \rho_c}, \quad (4)$$

where $r = R/R_0$ is the current dimensionless radius of the cylindrical front of carbon burning in the infinite cylindrical particle of char at the time τ .

In [20], the differential equation describing the burnout of fixed carbon from the char of the infinite plate with thickness $l = 2\delta_0$ (where δ_0 is the half-thickness of the plate) at a constant rate of carbon burning in the axial direction w_{ca} , was solved analytically. The equation for determining the time τ over which flat fronts of carbon burning shift from the initial position δ_0 on the char end faces and reach the current positions at a distance δ from the middle of the char plate was derived:

$$\tau = \frac{\rho_c}{w_{ca}}(\delta_0 - \delta). \quad (5)$$

The methodical difficulties of direct measurements of the carbon burning rate for the axial direction were noted, and a simplified approach for its estimation was proposed [20]:

$$w_{ca} = w_{cr} \frac{\rho_d}{\rho_{di}}, \quad (6)$$

where ρ_{di} is the initial density of dry biomass used for pellets pressing, kg/m³.

The current longitudinal coordinate δ of flat burning fronts at the time τ follows from the equation (5):

$$\delta = \delta_0 - \frac{\tau w_{ca}}{\rho_c}. \quad (7)$$

Dividing the right and left sides of the equation (7) by δ_0 , it was converted into a dimensionless form:

$$x = 1 - \frac{\tau w_{ca}}{\delta_0 \rho_c}, \quad (8)$$

where $x = \pm \frac{\delta}{\delta_0}$ are current longitudinal dimensionless coordinates of flat burning fronts in the infinite plate of char at a time τ .

According to obtained equations (4) and (8), the complete burnout of fixed carbon from the char of a cylindrical pellet occurs at the time when one of the dimensionless coordinates of burning fronts reaches zero value $\{r = 0 \cup x = 0\}$.

Determining the share of unburned fixed carbon in the char of a cylindrical pellet

After the volatile release, the mass of fixed carbon in the cylindrical particle of char per 1 m of its length is:

$$m_{cr,0} = \pi R_0^2 \rho_c. \quad (9)$$

At the current moment τ (from the beginning of fixed carbon burning), the mass of carbon in the infinite cylindrical particle of char per 1 m of its length is:

$$m_{cr} = \pi R^2 \rho_c. \quad (10)$$

The share of unburned carbon M_r in the burning infinite cylindrical particle of char to the time τ can be found as:

$$M_r = \frac{m_{cr}}{m_{cr,0}} = \frac{\pi R^2 \rho_c}{\pi R_0^2 \rho_c} = \frac{R^2}{R_0^2} = r^2. \quad (11)$$

After the volatile release, the mass of fixed carbon in the infinite plate of char per 1 m² of its area is:

$$m_{c\delta,0} = 2\delta_0 \rho_c. \quad (12)$$

At the current moment τ (from the beginning of the fixed carbon burning), the mass of carbon in the infinite plate of char per 1 m² of its area is:

$$m_{c\delta} = 2\delta \rho_c. \quad (13)$$

The share of unburned carbon M_x in the infinite plate of char to the time τ is:

$$M_x = \frac{m_{c\delta}}{m_{c\delta,0}} = \frac{2\delta \rho_c}{2\delta_0 \rho_c} = \frac{\delta}{\delta_0} = x. \quad (14)$$

The share of unburned carbon M , which remains in the char of the actual cylindrical pellet

to the time τ , was suggested to define as a product of unburned carbon shares for the infinite cylinder and the infinite plate:

$$M = M_r M_x = r^2 x. \quad (15)$$

The share of burnt fixed carbon to the time τ is:

$$C_\tau = 1 - M = 1 - r^2 x. \quad (16)$$

The share of carbon burned during the period from the time τ_1 to the time τ_2 can be defined as the difference of shares unburned carbon at corresponding moments.

Determining the pellet energy loss with unburned carbon of char

Because of the mechanical incompleteness of solid fuel combustion, its energy is partly lost. It is caused by the presence of unburned fuel in ash/slag, fallings through a grate, and flying ash. According to EN 15270:2007 [23] at pellets burning, the unburned fuel presence in the ash/slag is regarded. As to a char of a single pellet, only the carbon content in the ash causes energy loss because of incomplete mechanical combustion.

After the volatile release at the time $\tau = 0$, the mass of fixed carbon in the char of a single cylindrical pellet can be determined by an equation derived from material balances for processes of its drying and pyrolysis:

$$m_{cr\delta,0} = 2\pi R_0^2 \delta_0 \rho_c. \quad (17)$$

When pellet burning was terminated at the time τ counted from the beginning of carbon burning, the mass of unburned fixed carbon in the char of the single pellet, taking into account the above-disclosed mathematical description, is:

$$m_{cr\delta,\tau} = 2\pi R_0^2 \delta_0 \rho_c M. \quad (18)$$

The energy of the unburned carbon of the single pellet char until the time τ can be determined as:

$$Q_{uc} = q_c m_{cr\delta,\tau}, \quad (19)$$

where q_c is the heat value of carbon, J/kg.

The energy loss caused by incomplete combustion of the carbon of a single pellet can be estimated as:

$$q_{4a} = \frac{Q_{uc}}{m_w q_p}, \quad (20)$$

where q_p is the low heat value of pellets for 'as received state' J/kg; m_w is the mass of a single pellet for 'as received state', kg.

Experimental method

An experimental study of the carbon burnout from the pellet char was carried out by a single pellet burning in a heated muffle furnace with free access of air. The following features characterised the experiments. Pellets for research were picked out from industrial pellet batches. For the picked-out pellets, the moisture and ash content were determined following ISO 18134-2:2017 [24] and ISO 18122:2015 [25]. The density of single pellets in the 'as received state' and in the dry state was determined by the stereometric method described in ISO 18847:2016 [26]. The volatile content was determined as close to ISO 18123:2015 [27], but using whole pellets and their thermal decomposition in a stainless-steel crucible. Low heat values for each type of pellets q_p were estimated according to ISO 16993:2016 [28], but for really found contents of moisture W_{ar} and ash A_p , using typical low heat values for softwood and wheat straw given in ISO 17225-1:2014 [29].

Defectless pellets (correct cylindrical shape, no cracks) were selected for experiments; their ends were cut and polished to obtain samples in the form of rectangular cylinders. Prepared dried samples were weighed with an accuracy of ± 0.01 g, and their size was measured with an accuracy of ± 0.1 mm. For prepared samples, the rate of carbon burnout from char in the radial direction w_{cr} was measured according to the method described in [19]. The carbon burnout rate from char in the axial direction w_{ca} was estimated according to equation (6).

The pellet prepared for investigation was placed on a horizontal stainless-steel wire-gauze shelf with a 1 mm cell, placed at the support. The shelf was at 40 mm height above the support base.

The muffle furnace had a 200-mm-wide, 120-mm-high, and 300-mm-long internal space.

At the furnace aperture, a partition made of fire-proof bricks with a 60 × 70-mm window was installed, which ensured a reduction of heat losses and allowed bringing the mentioned support with the pellet to be investigated into the furnace. The furnace was equipped with a K-type thermocouple, the microprocessor temperature controller type RT-102 (JSC Lvivprylad, Ukraine), and a contactless switch in the electric heater circuit. Controller settings ensured the maintenance of the set furnace temperature with error margins $\pm 10^\circ\text{C}$. For the purposes of this paper, the experiments were carried out at a muffle temperature of 700°C .

The support with the pellet was placed into the preheated furnace so that the sample was at a distance of 80 mm from the muffle back wall. Free air access was provided to the furnace space for pellet burning through the open furnace door. The duration of carbon burnout was measured with a stopwatch as a period from the completion of volatile release until the end of carbon glowing inside the ash particle. The error of determining the duration of carbon burnout was: up to 3 s at the beginning of char burning and near 1 s after the completion of carbon burnout, up to 4 s in total.

After burning, the ash of straw pellets was grey as it contained carbon that did not burn out under experimental conditions. After experiments with burning pellets of the same type, ashes of all pellets used were collected. According to ISO 1171:2010 [30], the collected ash was heated in the muffle furnace at 815°C with moistened air purging through furnace space. The observed reduction of ash mass was accepted as the mass of oxidised carbon. A possible decrease in the ash mass due to high-temperature reactions and evaporation of light-melting components was neglected.

For each type of pellet used in experiments, carbon and ash balances for pyrolysis and fixed carbon burnout processes were made, and the initial mass of fixed carbon m_{cf} in the pellets used and the mass of residual unburnt carbon m_{uc} in the ash were defined. The share of the unburned fixed carbon remaining in the ash of pellets was calculated by the expression:

$$M = \frac{m_{ca}}{m_{cf}}. \quad (21)$$

RESULTS

For experimental studies, wheat straw pellets with a nominal diameter of 6 and 8 mm and wood pellets with a nominal diameter of 6 mm were used. The properties of these pellets are shown in the Table.

Dimensions of the char, formed from wood or straw pellet with a diameter of 6 mm were almost equal to those of the original pellet. The length of the char of the straw pellet with a diameter of 8 mm was close to that of the original pellet, but the diameter decreased slightly.

The dimensions of ash particles came up to 60–75% of the dimensions of initial pellets. The ash of the wood pellet had a loose structure and was easily destroyed when touched, and its colour was light brown indicating complete burn-out of carbon. For straw pellets, the more durable ash formed with a grey surface, and its breaking showed the black colour inside, which indicated incomplete carbon burnout. The structure of the straw pellet ash was loose with no signs of melting. For example, Fig. 2 contains photos of used wood and straw pellets 20 mm long and views of chars and ashes formed from them.

Table. Properties of pellets used in experiments

	Parameters	Unit	Straw pellets SPU-6	Straw pellets SPK-8E	Wood pellets WPCh-6
1	Nominal diameter, D	mm	6	8	6
2	Actual diameters, d	mm	5.8–6.0	8.0–8.3	6.0–6.3
3	Moisture content in bulk, W_{ar}	%wt.	7.45	8.80	7.92
4	Ash content in bulk, A_d	%wt.	5.45	7.65	0.40
5	Range of actual density of individual dry pellets	kg/m ³	1102–1305	987–1033	1063–1305
6	Average density of dry pellets used in experiments ρ_d	kg/m ³	1143	1010	1254
7	Accepted density of dry biomass used for pellets pressing ρ_{di}	kg/m ³	410	410	400
8	Volatile matter content, V_{daf}	%wt.	79.6	80.7	82.0
9	Rate of fixed carbon burnout in the radial direction, w_{cr}	g/(m ² ·s)	1.68	0.95	1.62
	Confidence interval of w_{cr} at significance coefficient $\alpha = 0.95$	g/(m ² ·s)	0.21	0.06	0.09
10	Estimated rate of fixed carbon burnout in the axial direction, w_{ca}	g/(m ² ·s)	5.13	2.34	5.1
11	Low heat value of pellets, q_p	kJ/kg	15950	15259	17365

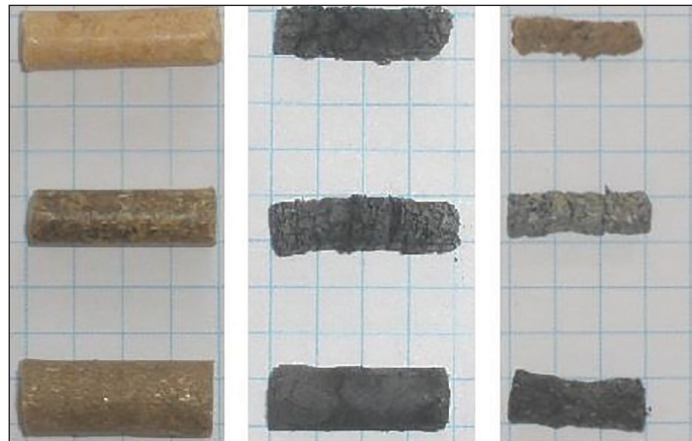


Fig. 2. Pellets (left), their chars (centre), and ashes (right), top down: a 6 mm wood pellet, a 6 mm straw pellet, an 8 mm straw pellet. The grid of the background paper is 5 mm

Ash of SPU-6 straw pellets contained 6.3% wt. of the unburned carbon, corresponding to the share of unburned fixed carbon $M = 0.016$; and that of SPK-8E 4.4% wt. of the unburned carbon and the share of unburned fixed carbon $M = 0.020$. The energy loss with unburned carbon for the SPU-6 straw pellets (diameter 6 mm) was estimated as $q_{4a} = 0.61\%$, and for the SPK-8E straw pellets (diameter 8 mm) $q_{4a} = 0.72\%$.

The experimental data of the duration of the burnout of fixed carbon from the char of

wood pellet (nominal diameter 6 mm, lengths from 2.5 to 42 mm) are shown in Fig. 3. The solid line shows the duration of complete carbon burnout from their char, which was calculated by equation (8), and the dashed line by equation (4). As the carbon burnout was complete, calculation of the burnout duration by equations (9)–(15) gave the same results.

The data in Figs 4 and 5 show the experimentally found duration of fixed carbon burnout from the char of the straw pellets SPU-6 (nominal

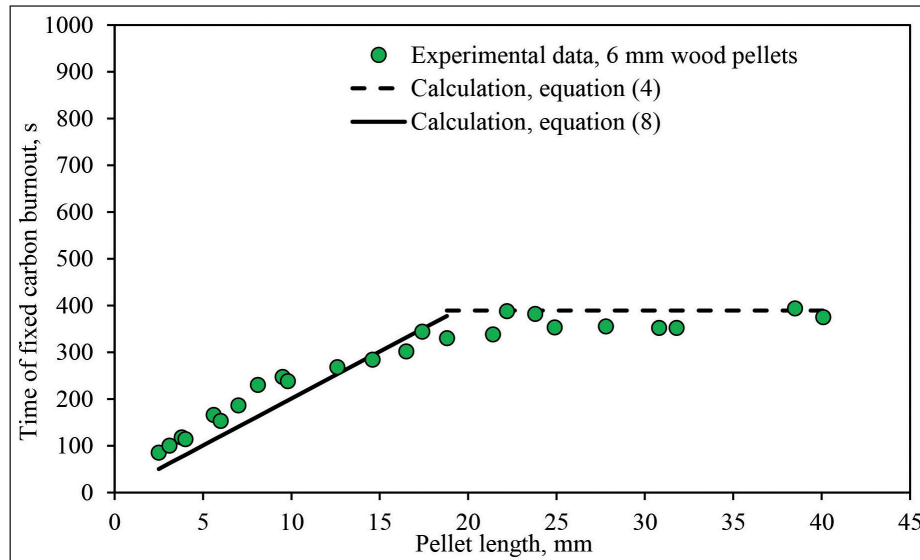


Fig. 3. The duration of the fixed carbon complete burnout from the char of a single wood pellet WPC-6 (diameter 6 mm) in the muffle furnace at 700°C and free air access depending on the pellet length

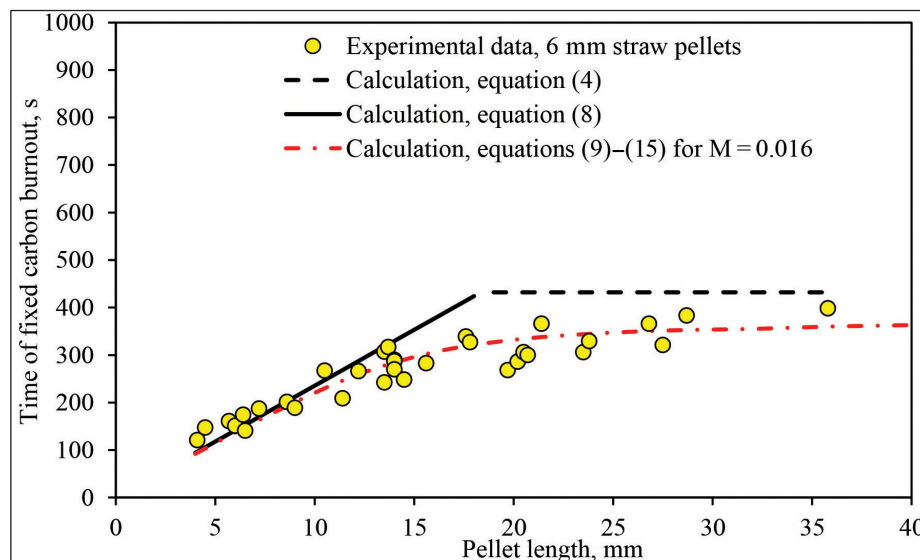


Fig. 4. The duration of the fixed carbon burnout from the char of a single straw pellets SPU-6 (diameter 6 mm) in the muffle furnace at 700°C and free air access depending on the pellet length

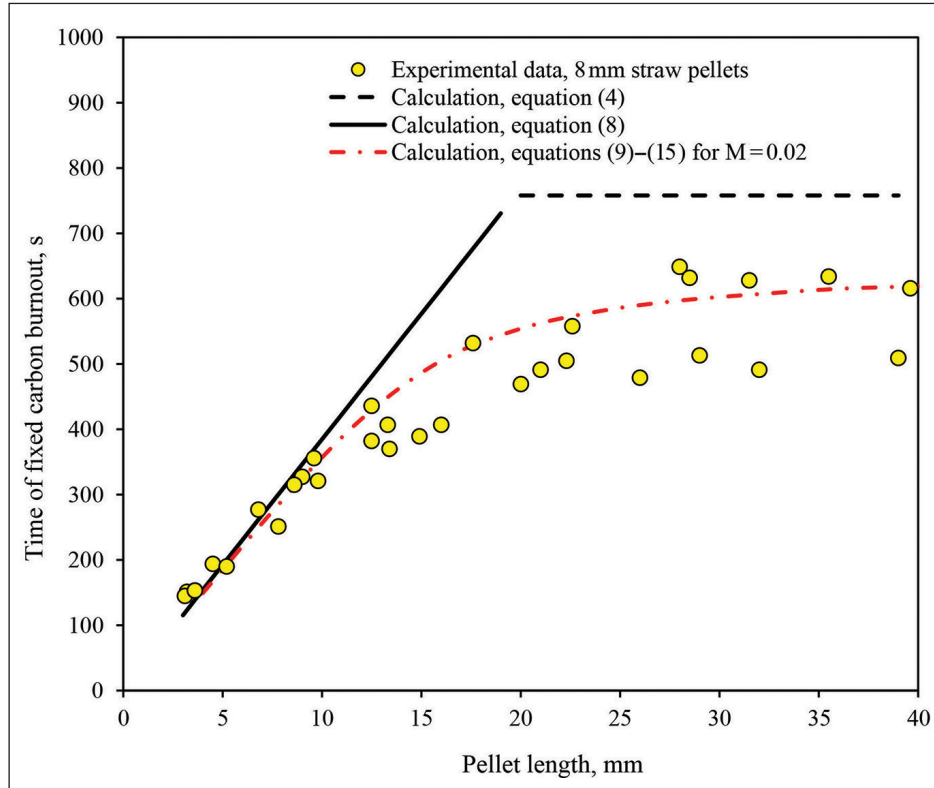


Fig. 5. The duration of the fixed carbon burnout from the char of the single straw pellets SPK-8E (diameter 8 mm) in the muffle furnace at 700°C and free air access depending on the pellet length

diameter 6 mm) and SPK-8E (nominal diameter 8 mm) depending on the pellet length. Here the solid line shows the duration of complete carbon burnout from the char of the same pellets calculated by equation (8), and the dashed line – according to equation (4). The dot-dash line represents the duration of fixed carbon incomplete burnout to reach the experimentally found share of unburned carbon M , calculated according to equations (9)–(15).

DISCUSSION

In Table, the difference between w_{cr} and w_{ca} is due to pellet anisotropy. Studying wood briquettes, Sova et al. [31] found that thermal conductivity along the briquette axis was (0.35 ... 0.45) W/(m·K) and almost three times lower – (0.13 ... 0.15) W/(m·K) – perpendicular to the axis. It is possible to assume that a similar anisotropy of thermal conductivity exists for pellets and char formed from pellets after volatile release. More intense thermal conductivity in the direction of the pellets axis provides more intensive heat flux from the burning front towards carbon in the adjacent layer, thus

accelerating its heating up. Then heated carbon reacts at a higher rate, provided sufficient oxygen is available.

The rate of fixed carbon burnout in the radial direction w_{cr} was measured at a furnace temperature of 700°C. According to the data in [16, 17], a burning particle of pellet char was overheated above furnace temperature; at that, the highest temperature at the particle surface was up to 800°C, and at the centre of char, it achieved 915°C by the moment of char burning completion. The measured rate of fixed carbon burnout in a radial direction w_{cr} is conditional. It characterises the burnout rate because of the complex influence of many factors: rapid heating up of pellet at placing into the furnace, diffusion of oxygen and reactions products, concentrations in the reaction zone, the rate of chemical reactions, heat transfer, and temperature change in the burning zone.

There was a complete burnout of fixed carbon from the char of the wood pellet at such low-temperature combustion, but carbon did not completely burn out from the straw pellet char. The residual carbon content was 4.4–6.6% in the ashes,

corresponding to the loss of 0.6–0.7% of the straw pellet energy. As recommended in [32], the allowable loss of wood fuel energy because of mechanical incompleteness of burning in boilers should not exceed 2%. This recommendation can be applied to similar solid biofuel, straw pellets. Therefore, the achieved residual content of unburnt fixed carbon in ashes can be considered acceptable for boiler burners at low-temperature combustion of straw pellets.

The data in Fig. 3 show a satisfactory coincidence of calculated and experimentally found durations of complete fixed carbon burnout from the char of wood pellets with a difference between them of up to 16%.

The data in Figs 4 and 5 show essential noncoincidence of calculated and experimentally found time (up to 21–39%) for reaching the experimentally achieved share of unburnt fixed carbon at low-temperature burning of straw pellet char. It should be mentioned that deviations have different directions and can be considered random. From the analysis of data in Figs 3, 4, and 5 follows that the inconsistency of the calculated and experimentally determined data cannot be explained by the maximum possible errors in measuring the length of pellets ± 0.1 mm and the burnout duration of ± 4 s. The following reasons can mainly cause revealed noncoincidence.

Graphs presented in Figs 3, 4, and 5 were calculated at average density for corresponding types of pellets. However, every single pellet was characterised by its density in the range shown in Table. Equations (1), (5), and (2) indicate more prolonged fixed carbon burnout with density increase. For 6 mm wood pellets WPCh-6, relative deviations of the actual density of individual pellets from the average density of these pellets were in range (–15% ... +4%), for 6 mm straw pellets SPU-6 in range (–4% ... +14%), and for 8 mm straw pellets SPK-8E in range (–3% ... +2%). So, the inconsistency of calculated and experimental data because of changing individual pellets density can partially explain observed noncoincidence.

In addition, individual pellets differ in density and the properties of fine particles from which they were pressed. According to the author's observations, denser morphological components of biomass, in particular wood knots and straw nodes, burn out slower. The accidental presence of fine

particles from such dense components in the pellet can cause its more prolonged burnout. Based on this, the difference in the duration of carbon burnout from pellets of almost identical length and mass can be explained. For the same reason, the experimentally determined rate of carbon burnout is characterised by the average value and confidence interval (Table). Equations (4) and (15) indicate the sensitivity of the estimated duration of fixed carbon burnout to changes in the value of the burnout rate w_{cr} , as it is indirectly included with the second power.

Thus, the duration of the burnout of fixed carbon from pellets depends also on uncontrolled stochastic factors. Therefore, when using the average characteristics of pellets, calculations according to the proposed dependencies give results close to the most likely value of the duration of burnout of a large number of pellets of a given length. The values for individual pellets will differ from the most likely value to the extent that their properties differ from the average value. For the pellets of a given length, the variability of their properties requires a separate study.

Because of the influence of uncontrolled factors, statistical analysis methods can be applied for the comparison of experimental and calculated data [33–35]. The determination coefficients R-squared for sets of experimental and calculated durations of fixed carbon burnout were 0.96, 0.87, and 0.91 for wood pellets WPCh-6, straw pellets SPU-6, and SPK-8E, respectively.

The high values of R-squared indicate that the analytically obtained solutions reflect the relationship between the sought and the taken into account defining values in the mathematical description of the fixed carbon burnout from the char of pellets. The value of the determination coefficient can be interpreted as follows: 0.96, 0.87, and 0.91 of variances in the duration of burnout for the corresponding pellets can be explained by factors taken into account in the mathematical description of the process, but 0.04, 0.13, and 0.09 of variances are due to other factors that were not taken into account and to measurement errors.

Comparison of dependencies (4) and (8) showed that calculated durations of carbon burnout from the pellet char in radial and axial directions should be the same at the pellet length, which featured a critical l_{cr} :

$$l_{cr} = d \left(\frac{w_{ca}}{w_{cr}} \right). \quad (22)$$

Critical lengths for studied wood and straw pellets were (18.4 ... 19.7) mm, so approximately it can be considered $l_{cr} = 20$ mm. For example, in Fig. 6, the calculated dimensionless coordinates of carbon burning fronts r , x and the share of unburned fixed carbon M are shown for straw pellets, having a diameter of 8 mm, at lengths 10 mm and 30 mm. From the presented data, it follows that for shorter pellets $l < l_{cr}$: $x \rightarrow 0$ faster than r , so the burnout of a shorter pellet is controlled by its burnout in the axial direction (Fig. 6a), and for a longer pellet $l > l_{cr}$: $r \rightarrow 0$ faster than x , so the burnout of a longer pellet is controlled by its burnout in the radial direction (Fig. 6b).

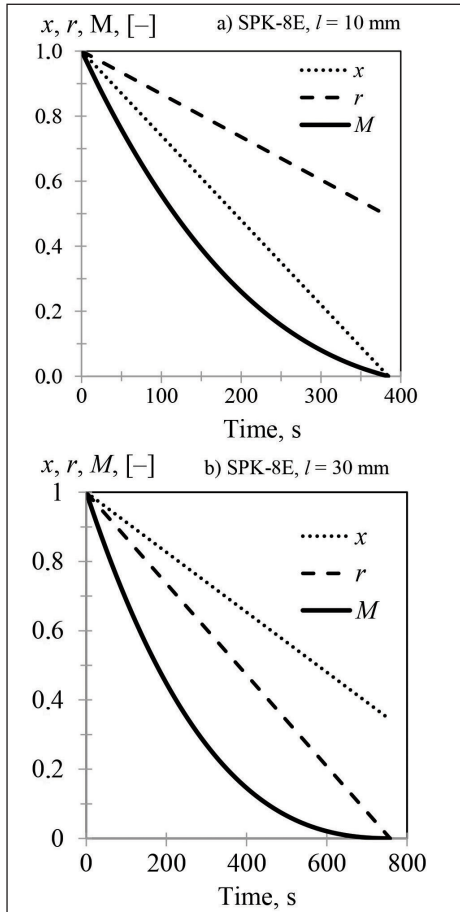


Fig. 6. The calculated dimensionless coordinates of carbon burning fronts r and x , and the share of unburned fixed carbon M at burning straw pellets SPK-8E, diameter 8 mm, at (a) pellet length $l = 10$ mm; (b) pellet length $l = 30$ mm

As it was defined by the standard EN 14588:2010 [36], pellets can have an arbitrary length in the range from 3.15 to 20 mm, but according to the currently valid standard ISO 16559:2014 [37] for pellets, with a diameter 6 mm and 8 mm, the length can be in the wider range from 3.15 to 40 mm. Thus, according to standards, pellets may differ in length.

According to the results found, the duration of fixed carbon burnout for the long pellets (30–40 mm) was more than three times longer than that for the shortest pellets. The practical importance of the presented study is the following: the usage of ‘short’ pellets, which are characterised by a faster burnout rate in the axial direction, may become purposeful for intensive burning. On the contrary, for slowing down burning, especially to arrange low-temperature burning of straw pellets, it may be feasible to use ‘long’ pellets for which the carbon burnout duration is determined by slower burnout rate in the radial direction.

CONCLUSIONS

Described experimental results allowed concluding that the low-temperature burning of single straw pellets at a muffle furnace temperature of 700°C, with the formation of loose ash without signs of melting was possible.

The proposed mathematical description of the fixed carbon burnout from the char of a single cylindrical pellet at free air access takes into account the different rates of carbon burnout in axial and radial directions. Analytically obtained equations determine the radial and axial coordinates of the carbon burning fronts in dimensional and dimensionless forms. The dependencies, which describe the share of unburned fixed carbon that changes in time, allow estimating the pellet energy loss because of incomplete carbon burnout. Calculations of the duration of fixed carbon burnout from char of straw and wood pellets are in acceptable accordance with experimental data.

The proposed mathematical description and obtained dependencies can be used to calculate carbon burnout from the char of a single cylindrical pellet or rarely distributed monofractional pellets at free air access. Studying carbon burnout from actual industrial pellets containing particles of different lengths may be the next step in research.

The most noteworthy research finding is that for long pellets, the fixed carbon burnout is controlled mainly by its slower burnout rate in the radial direction, and for short pellets by a more intensive burnout rate in the axial direction.

The practical value of the results obtained is that the use of shorter pellets, which are characterised by faster burnout, may become purposeful for intensive burning. On the contrary, for slowing down burning, especially to arrange low-temperature burning of straw pellets, it may be feasible to use longer pellets with extended burnout. In studied conditions, despite unburned carbon presence in the ash of straw pellets, losses of the pellet energy with unburned carbon were estimated as 0.61–0.72%, which is acceptable for boiler burners.

Received 30 May 2021

Accepted 4 May 2022

References

1. Energetychna stratehiia Ukrainy na period do 2035 roku 'Bezpeka, energetychna efektyvnist, konkurentospromozhnist. Kabinet Ministriv Ukrainy, rozporiadzhennia 605-r vid 18 serpnia 2017. [Energy strategy of Ukraine for the period till year 2035 "Safety, energy efficiency, competitiveness." Council of Ministers of Ukraine. Order 605-r of 18 august 2017]. <https://zakon.rada.gov.ua/laws/show/605-2017-p?lang=en>. Ukrainian.
2. Energy consumption from renewable sources for 2007–2017. State statistics service of Ukraine. http://www.ukrstat.gov.ua/operativ/operativ2016/sg/ekolog/eng/esp_vg_e.htm
3. Energy balance of Ukraine, 2017 (by products); http://www.ukrstat.gov.ua/operativ/operativ2014/energ/en_bal_prod/Bal_prod_2017_e.xls
4. Geletukha G., Zheliezna T., Zhovmir M., Matveev Yu., Drozdova O. Assessment of biomass potential in Ukraine. Part 2. Energy crops, liquid biofuels, biogas. *Industrial heat engineering*. 2011. Vol. 33. No. 1. P. 57–64. <http://dspace.nbu.gov.ua/handle/123456789/60302>. Ukrainian.
5. Phyllis 2. Database for biomass and waste. <https://phyllis.nl>
6. Wopienka E., Carvalho L., Ohman M., Schwabl M., Hastlinger W. Evaluation of ash melting behaviour of solid biomass based on fuel analyses. *19th European Biomass Conference and Exhibition*, Berlin, 2011. P. 1283–1286. doi:10.5071/19thEU-BCE2011-VP2.1.24.
7. Jandačka J., Holubčík M., Papučik Š., Nosek R. Combustion of pellets from wheat straw. *Acta Montanistica Slovaca*. 2012. Vol. 17. No. 4. P. 283–289. Available at: <https://pdfs.semanticscholar.org/f0a0/a16acb881e5f7f9d3c388775a0c46ba0579f.pdf>
8. Biagini E., Tognotti L. Comparison of devolatilization/char oxidization and direct oxidization of solid fuels at low heating rate. *Energy & Fuels*. 2006. Vol. 20. P. 986–992. doi: 10.1021/ef0503156.
9. Dunayevska N., Zasiadko Ya., Shchudlo T. Thermal destruction kinetics of coal and solid biomass mixtures. *Ukrainian Food Journal*. 2018. Vol. 7. No. 4. P. 738–753. doi: 10.24263/2304-974X-2018-7-4-17.
10. Dunayevska N., Chernyavskiy M., Shchudlo T. Co-combustion of solid biomass in pulverized anthracite-coal firing boilers. *Ukrainian Food Journal*. 2016. Vol. 5. No. 4. P. 748–764. doi: 10.24263/2304-974X-2016-5-4-14.
11. Karp I., Pyanykh K. Substitution of natural gas by biomass. *The Advanced Science Journal*. Vol. 2014. No. 7. P. 60–66. doi: 10.15550/ASJ.2014.07.060.
12. Yang Y. B., Sharifi V. N., Swithenbank J. Numerical simulation of the burning characteristics of thermally-thick biomass fuels in packed-beds. *Transactions of Institution of Chemical Engineers, Process Safety and Environmental Protection*. 2005. Vol. 83. No. 6. P. 549–558. doi: 10.1205/psep.04284.
13. Lu H., Robert W., Peirce G., Ripa B., Baxter L. Comprehensive study of biomass particle combustion. *Energy & Fuels*. 2008. Vol. 22. No. 4. P. 2826–2839. doi: 10.1021/ef800006z
14. Mehrabian R., Zahirovic S., Scharler R., Obernberger I., Kleditzsch S., Wirtz S., Scherer V., Lu H., Baxter L. L. A CFD model for thermal conversion of thermally thick biomass particles. *Fuel Processing Technology*. 2012. Vol. 95. P. 96–108. doi: 10.1016/j.fuproc.2011.11.021.
15. Momeni M., Yin C., Kær S. K., Hansen T. B., Jensen P. A., Glarborg P. Experimental study on effects of particle shape and operating conditions on combustion characteristics of single biomass particles. *Energy & Fuels*. 2013. Vol. 27. No. 1. P. 507–514. doi: 10.1021/ef301343q.

16. Zhovmir M. Temperature of wood and straw pellets at carbon burning out. *Vidnovliuvana enerhetyka*. 2017. No. 3. P. 87–95. Ukrainian. Available at: <https://ve.org.ua/index.php/journal/article/view/46/34>.
17. Silin V. E., Ryzhkov A. F., Nadir S. M. Sh. Low-temperature biomass combustion. *Energy technologies and resource saving*. 2008. No. 5. P. 9–15. Russian.
18. Palchonok G., Leckner B., Tullin C., Martinsson L., Borodulya A. Combustion characteristics of wood pellets. *Proceedings of the 1st World Pellet Conference*. Stockholm. 2002. P. 105–106.
19. Zhovmir M. Kinetics of thermolysis and burning of solid biofuels particles. Part 3. Burning out rate of cokeash residue of wood and straw pellets. *Vidnovliuvana enerhetyka*. 2016. No. 4. P. 86–93. Ukrainian. Available at: <https://ve.org.ua/index.php/journal/article/view/111/68>.
20. Zhovmir M. Kinetics of thermolysis and burning of solid biofuels particles. Part 4. Influence of pellets anisotropy on oxidization rate of carbon from coke ash residue in axial and radial direction. *Vidnovliuvana enerhetyka*. 2017. No. 4. P. 93–100. Ukrainian. Available at: <https://ve.org.ua/index.php/journal/article/view/29/21>.
21. Wendi Guo, Lim C. J., Sokhansanj S., Bi X., Melin S. Thermal conductivity of wood pellets. *Fuel*. 2013. Vol. 103. P. 347–355. doi: 10.1016/j.fuel.2012.08.037.
22. Paulauskas R., Džiugys A., Striūgas N., Garšvinskaitė L., Misiulis E. Experimental and theoretical investigation of wood pellet shrinkage during pyrolysis. *Energetika*. 2014. Vol. 60. No. 1. P. 1–11. doi: 10.6001/energetika.v60i1.2867.
23. EN 15270:2007. Pellet burners for small heating boilers – Definitions, requirements, testing, marking. European Committee for Standardization. 2007, 49 p.
24. ISO 18134-2:2017. Solid biofuels – Determination of moisture content – Oven dry method – Part 2: Total moisture – Simplified method. Geneva, ISO, 2017, 5 p.
25. ISO 18122:2015. Solid biofuels – Determination of ash content. Geneva, ISO, 2015, 6 p.
26. ISO 18847:2016. Solid biofuels – Determination of particle density. Geneva, ISO, 2016, 12 p.
27. ISO 18123:2015(en). Solid biofuels – Determination of the content of volatile matter. Geneva, ISO, 2015, 16 p.
28. ISO 16993:2016. Solid biofuels – Conversion of analytical results from one basis to another. Geneva, ISO, 2016, 10 p.
29. ISO 17225-1:2014. Solid biofuels – Fuel specifications and classes – Part 1: General requirements. Geneva, ISO, 2014, 64 p.
30. ISO 1171:2010. Solid mineral fuels – Determination of ash. Geneva, ISO, 2010, 4 p.
31. Sova D., Porojan M., Bedeleian B., Humnic G. Effective thermal conductivity models applied to wood briquettes. *International Journal of Thermal Sciences*. 2018. Vol. 124. P. 1–12. doi: 10.1016/j.ijthermalsci.2017.09.020.
32. The thermal calculation of boiler units (Normative method). Edition of Kuznetsov N. V. et al. 2nd ed. Moscow. Publishing house ‘Energy’. 1973. 296 p. Russian.
33. Kutner M. H., Nachtsheim C. J., Neter J., Li W. *Applied Linear Statistical Models*. Fifth Edition. McGraw-Hill/Irwin. 2005. 1396 p.
34. Chicco D, Warrens M. J., Jurman G. The coefficient of determination R-squared is more informative than SMAPE, MAE, MAPE, MSE and RMSE in regression analysis evaluation. *PeerJ Computer Science*. 2021. No. 7: e623. doi.org/10.7717/peerj-cs.623
35. Gupta V. *Regression explained in simple terms. SPSS for beginners*. VJ Books Inc. 2000. 24 p.
36. EN 14588:2010. Solid biofuels – Terminology, definitions and descriptions. European Committee for Standardization. 2010, 42 p.
37. ISO 16559:2014. Solid biofuels – Terminology, definitions and descriptions. Geneva, ISO, 2014, 32 p.

Mykola M. Zhovmir

ANGLIES IŠDEGIMAS IŠ VIENOS CILINDRINĖS GRANULĖS NUODEGŲ